Research article

Enhancing Digital Elevation Model Accuracy for Flood Modelling – A Case Study of the Ciberes River in Cirebon, Indonesia

Sahid Sahid[*]

Faculty of Regional and Infrastructure Technology, Institut Teknologi Sumatera, Lampung 35365, Indonesia

[*] Correspondence: sahid@pariwisata.itera.ac.id

Abstract

Topographic conditions represented by the Digital Elevation Model (DEM) are essential in flood inundation models. The DEM, which is categorised as a Digital Surface Model (DSM) stores the height information, besides the ground and non-ground elevation required for preprocessing before being employed in hydrologic applications, particularly in relation to flood modelling by removing non-ground elevation along the floodplain and river channels. The improvement in the accuracy of flood inundation modelling is crucial in reducing the impact of flood disasters. This study aims to compare the accuracy level of the DEM based on TerraSAR-X data with the filtering process using slope-based filtering and combining the cross-sectional river profile from the field measurement with the filtered DEM. The result confirms that the accuracy of the DEM product is improved via filtering to remove non-ground elevations, and there is a significant improvement in accuracy by means of fused river profile information for the filtered DEM. The results of adding river information to the DEM could provide a representation closer to the cross-sectional profile of the river based on field measurements within the accuracy level Mean Absolute Error 2.51 m, 2.72 m, and 1.91 m in the left overbank, right overbank and centre of the river, respectively. The performance results of the 2-dimensional flood hydrodynamic modelling using HEC-RAS derived from the DEM before filtering, after filtering, and the addition of river information show increasing accuracy in flood depth at each stage of the DEM processing. There is an improvement in accuracy in flood depth of approximately 11.67% using the filtered DEM, besides an increase in accuracy in flood depth by 24.98% utilising the filtered DEM with added river channel information.

Keywords: enhancing DEM; digital elevation model; DEM filtering; digital surface model; slope-based filtering.

1. Introduction

Flood events occur when water overflows the capacity of river channels due to rainfall intensity, topographic conditions, soil infiltration capacity, and land cover type. Flood disasters classified as hydro-meteorological hazards generate highly destructive power globally (Sarkar & Mondal, 2020). Based on the flood disaster data available in Indonesia, over the past 15 years (1998-2022), has been an increasing trend concerning disasters, with the highest increase in the number of flood disasters occurring in 2020, with a percentage increase of 104% (BNPB, 2023). The increase in the number of flood disasters is accompanied by a rise in the number of people affected and damage to property and resources. In 2020, 1,531 flood events in Indonesia resulted in 4,624,979 victims, including 132 fatalities, 15 missing, 64 injured, 3,843,714 affected, 781,054 displaced, and damage to 30,649 facilities (BNPB, 2023). Another severe impact of flood disasters is the prolonged and prevailing impact that affects the physical and psychological health (posttraumatic) of the victims (Carra & Curtin, 2017; Fernandez *et al.,* 2015; Stephenson *et al.,* 2014).

Overall, floods exhibit highly destructive power and cause loss of life and damage to property. In recent years, the frequency of flood disasters has been increasing owing to the influence of climate change, which has generated a rise in the earth's surface temperature, related to atmospheric warming, which is associated with natural disasters such as floods (Cloke, 2013; Kun-dzewicz *et al.,* 2014). Alfieri et al. (2017) simulated scenarios of 1.5°C, 2°C and 4°C increases in the earth's surface temperature. The results obtained exhibited a positive relationship between global warming and future flood risk. Additional climate change scenarios were conducted by Hirabayashi *et al.* (2013). The research established that the frequency of flood events in the Asian region will experience a significant increase. Xafoulis *et al.* (2023) asserted that climate change is causing an increase in the frequency and intensity of flood events. Without implementing adequate mitigation measures, the rise in the frequency of flood events will substantially impact the resulting losses. Flood modelling, recognised for its high precision, is a suitable mitigation measure to reduce the losses stemming from flood incidents.

Flood modelling is fundamental in mitigating the impact of flood disasters, which are a highly destructive force and are likely to increase in frequency. Identifying potentially flooded areas is the first step in mapping flood-prone areas. Predicting and mapping flood hazards remains a

challenge owing to factors such as the roughness of the surface flow (Ardıçlıoğlu & Kuriqi, 2019), the complexity of river geomorphology (Kuriqi *et al.,* 2020), the availability of flood flow data and detailed topographic data (Casas *et al.,* 2006; Muthusamy *et al.,* 2021). The accuracy of flood inundation distribution resulting from modelling depends on the topographic data's level of detail and descriptiveness. Digital elevation model (DEM) data, which acts as topography input data, is a crucial element in accurately modelling flood inundation for both river channels and floodplains (Casas *et al.,* 2006; Muthusamy *et al.,* 2021). Currently, DEM data is extensively available to support flood inundation modelling, including open data sources that can be accessed for free, such as SRTM, ASTER GDEM, Sentinel, ALOS and Indonesia's very own DEMNAS (Ihsan & Sahid, 2021; Sahid *et al.,* 2017).

Researchers have previously implemented the use of DEM data from various sources to obtain hydrologic information and assess the accuracy of each type of DEM (Chymyrov, 2021; Tran *et al.,* 2023). Chymyrov (2021) compared three DEM Products, specifically AW3D30, ASTER v. 3, and SRTMGL1, used to assess the accuracy level in unearthing data regarding hydrological information pertaining to mountainous regions. The results indicate that the extraction of hydrological information based on the DEM product mentioned needs to be modified by utilising remote sensing data with a more detailed spatial resolution to obtain the hydrological boundaries matched to the field condition. Consistent with this, the use of DEM data with a lower resolution should be carefully considered as regards obtaining hydrological data, for instance, the delineation of river basins and their networks in lowland areas, as DEM products with a lower resolution do not provide information that aligns with reference data in lowland areas (Tran *et al.,* 2023). However, open DEM data sources have limited spatial resolution, indicating that a substantial amount of information on river channels and floodplains is generalised and may not accurately represent the original topography. Xafoulis *et al.* (2023) evaluated the application of the DEM based on the spatial resolution 5 m, 2 m from Hellenic Cadastre (HC) and 0.05 m from an Unmanned Aerial Vehicle (UAV) to perform flood simulation. The results indicate that DEM must consider adding river centre line information regarding the river channel, and the river must be calibrated based on satellite imagery with the aim of securing an ideal flood simulation. To acquire accurate flood modelling, the DEM as input data needs to be corrected by employing several approaches, namely DEM Editing, a newly developed DEM created with improved remote sensing technologies and the stochastic simulation of DEMs (Hawker *et al.,* 2018). Higher resolution DEMs may also result in bias in the river channel information concerning surrounding areas (Muthusamy *et al.,* 2021). More detailed DEM data, such as LiDAR data which can provide a detailed spatial resolution of the surface, is more expensive. When applying DEM data, it is essential to consider that it is a Digital Surface Model (DSM) product and not a Digital Terrain Model (DTM). DSM data is a DEM that stores information regarding the height of the earth's surface based on the coverings above it and not the original ground elevation (bare earth). The DSM provides information on the height of land and building coverings as well as the bare earth when the area is open (Danoedoro *et al.,* 2022). Additionally, DEM data does not accommodate underwater information, signifying that the data does not depict river morphology information. Therefore, it would be challenging to accurately estimate the extent of water discharge that would cause flooding when conducting flood modelling.

Based on the abovementioned reasons, this research aims to provide an alternative pre-processing method for DEM data prior to use in flood hydrodynamic modelling. The alternative method involves testing the accuracy of the DEM data against accurate reference data to obtain the accuracy level of the elevation data. After obtaining the accuracy level, data filtering is performed to remove non-ground elevation. Likewise, channel information is added by integrating the DEM data with river cross-section values. The preprocessing process completed on DEM data with less detailed resolution as input data in flood modelling is expected to produce accurate flood inundation modelling.

2. Research Methods

2.1. Study Area and Materials

The research was conducted in the Ciberes River segment located in the Ciberes Watershed Cirebon, West Java Province, Indonesia. Geographically, the Ciberes Watershed is located between 6° 58' 56.99" S and 6° 48' 22.06" S and 108° 32' 59.58" E to 108° 44' 48.90" E with a total area of approximately 118.88 km2. The selection of the river segment location was due to frequent flooding in the middle segment of the Ciberes River, which starts from the Ambit Dam up to 3.1 km along the river (Figure 1). The Ciberes Watershed has varying topographic conditions from upstream to downstream. The highest elevation in the upstream area has a height of approximately 300 metres above sea level, located in Kuningan Regency, while the middle and downstream areas

have relatively flat topographic conditions with heights ranging from 40-160 metres. The flat topographic condition in the middle of the river causes frequent flooding during the rainy season. Six flood disasters were recorded in 2022, attributable to the overflow of the Ciberes River (BNPB, 2023). The Ciberes River annually experiences flooding attributable to the intense rainfall. The Ciberes River, located in the Cirebon Regency, is an area that is susceptible to flood disasters, as stated in the report published by the National Disaster Management Agency, which mentions that the flood risk class in Cirebon Regency is high (BNPB, 2022).

The availability of data is a key factor in the success of research. The data utilised in this study consists of TerraSAR-X DEM data and 1:25,000 scale Topographic Maps of Indonesia obtained from the Geospatial Information Agency (BIG), as well as High-Resolution Satellite Image SPOT 7 data acquired on August 10, 2016 obtained from the National Institute of Aeronautics and Space of Indonesia (LAPAN). Moreover, river profile data and landcover data acquired from the Cimanuk-Cisanggarung River Basin Agency (CCRBA) were used to assess the comparison of elevations obtained from the river profile generated from the DEM data and field measurements and to roughness coefficients performing flood modelling. Additional data applied in this study is soil classification based on the Cirebon Regional Planning Agency. The river profile data obtained from the CCRBA were collected in 2017. The use of TerraSAR-X DEM data is due to its sufficiently detailed spatial resolution of 9 m, which can accurately depict the river channel in the study area. SPOT 7 satellite imagery, corrected, orthorectified, and sharpened with a spatial resolution of 1.5 m, was employed to delineate the study area's river body. ArcGIS, ENVI, and SAGA GIS software were used to perform the analysis and map presentation.
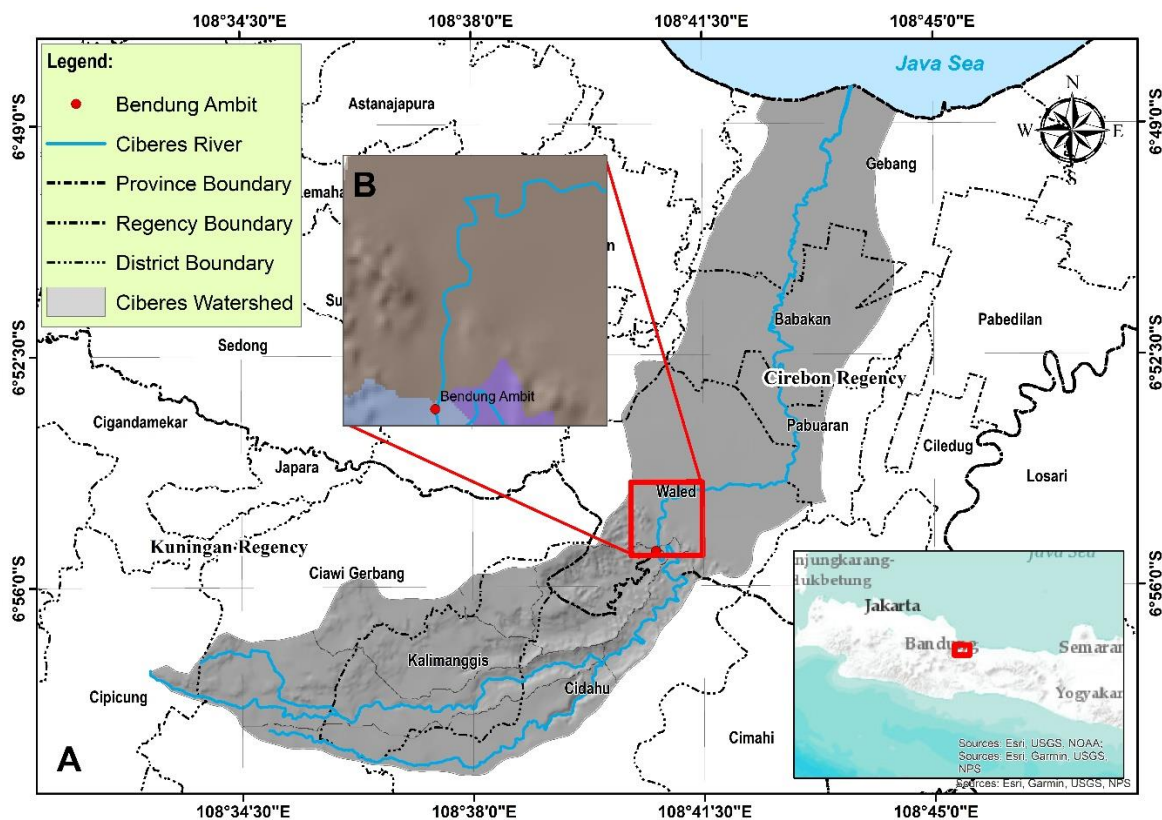

Figure 1. Study area of Ciberes River.

2.2. Data Analysis

2.2.1 Digital Elevation Model Filtering

The DEM data utilised in this study is TerraSAR-X data derived from Synthetic Aperture Radar (SAR) satellite imagery with a spatial resolution of 9 m x 9 m. The data has been orthorectified using the UTM Zone 49 S coordinate system. Confirming the projected coordinate system of the DEM data is essential to avoid location errors that may cause inaccuracies in the analysis. TerraSAR-X data is recognised as a DSM product. Hence, in flood inundation modelling, filter-ing is crucial to eliminate non-original ground elevations that can affect water flow distribution (Figure 2).
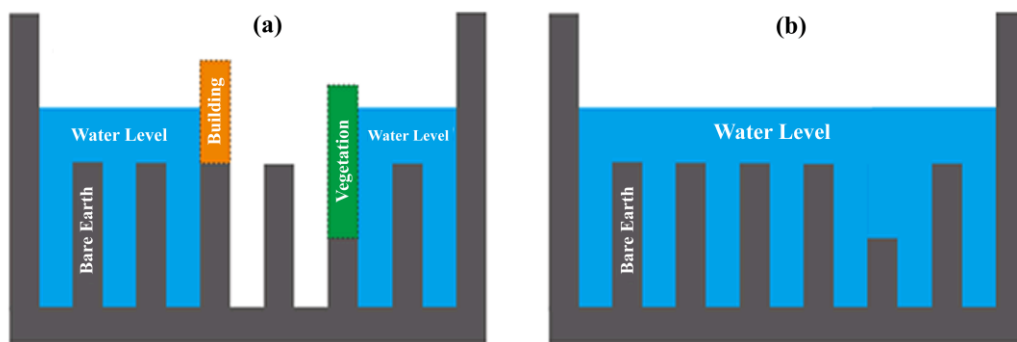
Figure 2. The water propagation process in hydrological flood modelling performance (a) illustrates a DSM that still provides information on building height and land cover in its data, (b) shows DEM data that has been filtered.

The elimination of non-ground points was achieved using the Vosselman approach, slope-based filtering (SBF), which considers slope-based ground surface elevation. SBF takes into account that a significant difference in elevation between two nearby points cannot be due to steep ground but is more likely because of the difference between the bare earth and the objects on top of it (Vosselman, 2000; Vosselman & Maas, 2001). The filtering is based on slope thresholds that determine if the slope difference between two neighbouring elevation points exceeds a threshold value (Sithole, 2001). The SBF method has two important parameters: the slope threshold and the kernel radius, or the range of objects considered non-ground points. The kernel radius should consider the size of the objects to be removed (Vosselman, 2000). The SBF analysis in the SAGA v.2.3.2 application performed the filtering process. After filtering, the Multilevel B-Spline Interpolation was used to complete the elevation values around the elevation points to generate the DEM data.

2.2.2. Vertical Bias Correction

Vertical accuracy is calculated to determine the level of precision of the elevation values (z) in the DEM before and after filtering. The vertical accuracy test is conducted by calculating the Root Mean Square Error (RMSE) (Equations 1) and Mean Absolute Error (MAE) (Equations 2) values of the elevation data of each DEM compared to reference data from high point sources from the Topographic map within a Scale of 1:25,000. RBI maps are employed as reference data because the high points generated are sourced from detailed scale aerial photo calculations and have been tested for accuracy. The RBI map has a vertical accuracy of half the contour interval value (12.5 m), therefore, the height accuracy level is 6.5 m (Specifications for Presenting Maps - Part 2: Scale 1:25,000, 2010). Accuracy testing that compares DEM data with reference data should have greater accuracy (Elkhrachy, 2017).

$$RMSE = \sqrt{\frac{\sum_{i-1}^{N}(H_{DEM}^i - H_{ref}^i)}{N}} \tag{1}$$

$$MAE = n^{n-1}\sum_{i-1}^{n}|P_i - O_i| \tag{2}$$

RMSE is the root mean square error, Hiref is the reference height value of the RBI high point, H i DEM is the height value of the DEM, and N is the total number of field sample points. MAE is the mean absolute error, n is the number of observations, P is the predicted value and O is the observed value. Furthermore, after the RMSE value is calculated, accuracy testing is also carried out by calculating the linear error confidence level (LE) at 90%, which is 1.65. LE90 is a matrix of the DEM error levels that can be measured to test the overall accuracy level of the DEM (Equation 3). Where accuracy is the elevation accuracy, E90 is the multiplying factor/90% confidence level, and RMSE is the root mean square error value.

$$Accuracy = E90 \ x \ RMSE \tag{3}$$

2.2.2. Fusion River Information to DEM

The additional riverbed information in the DEM is essential to obtain detailed cross-sections of the river, enabling the capacity of the river to be calculated accurately. Cross-section data (CS) consisting of lines and point locations (x and y) with elevation attribute values (m) from field measurements are used to compare the height accuracy level between the filtered DEM and the field measurement data. Prior to conducting accuracy testing, identification of the left and right edges of the river is required to determine the exact location of the river area (Gichamo *et al.,*

2012). Based on visual interpretation, the delineation of information pertaining to the river's edge (Left overbank, centre, right overbank) is obtained by overlaying the SPOT 7 satellite imagery with the same coordinate system as the DEM data. It is sharpened using the Gram-Schmidt Pan-Sharpening method. The Gram-Schmidt sharpening method is chosen because it maintains the number of bands in the image by combining multi-spectral and panchromatic images to obtain an image resolution of 1.5 m x 1.5 m. Image data processing is undertaken using the ENVI 5.3 image processing application. Image sharpening is performed to acquire detailed appearances of the river authority area, making it easier to delineate river information. Simultaneously, information on the central area of the river is obtained from the lowest elevation value obtained from field measurement data related to the river cross-section. The delineation process of the left, right, and central river lines is carried out using the ArcGIS 10.4 application.

The accuracy assessment is based on comparing the elevation values of the river's centre line, right overbank, and left overbank obtained from field measurements using the elevation values extracted from the filtered DEM. The accuracy is tested by calculating the RMSE and MAE values to determine the level of elevation differences in each part of the river. Moreover, the river body area information is incorporated into the DEM to obtain the accuracy level values of the three river sections. This requires subtracting the elevation values with the MAE calculation results at each height point passed by the river's three sections after the filtered DEM is converted into elevation point data (Figure 3). Two methods are applied to determine the points included in the three sections of the river. First, a 1-metre-wide buffer is applied to the delineated right and left riverbank lines so that the elevation points within the left and right buffer areas are assumed to be in the respective areas. Next, the elevation points located between the right and left banks of the river, which are assumed to be in the centre of the river, are reduced in height with the accuracy test results. After obtaining the filtered DEM elevation points subjected to elevation reduction on the right, left and central parts of the river, the elevation points attained from the river cross-section measurements are added before the elevation point data is converted back into the DEM. Adding elevation points from field measurements of the river cross-sections is intended to add detailed information concerning the river body. Re-interpolation to obtain DEM data from adding river body information is completed using the multilevel B-spline interpolation method, performed with the assistance of the SAGA GIS application.
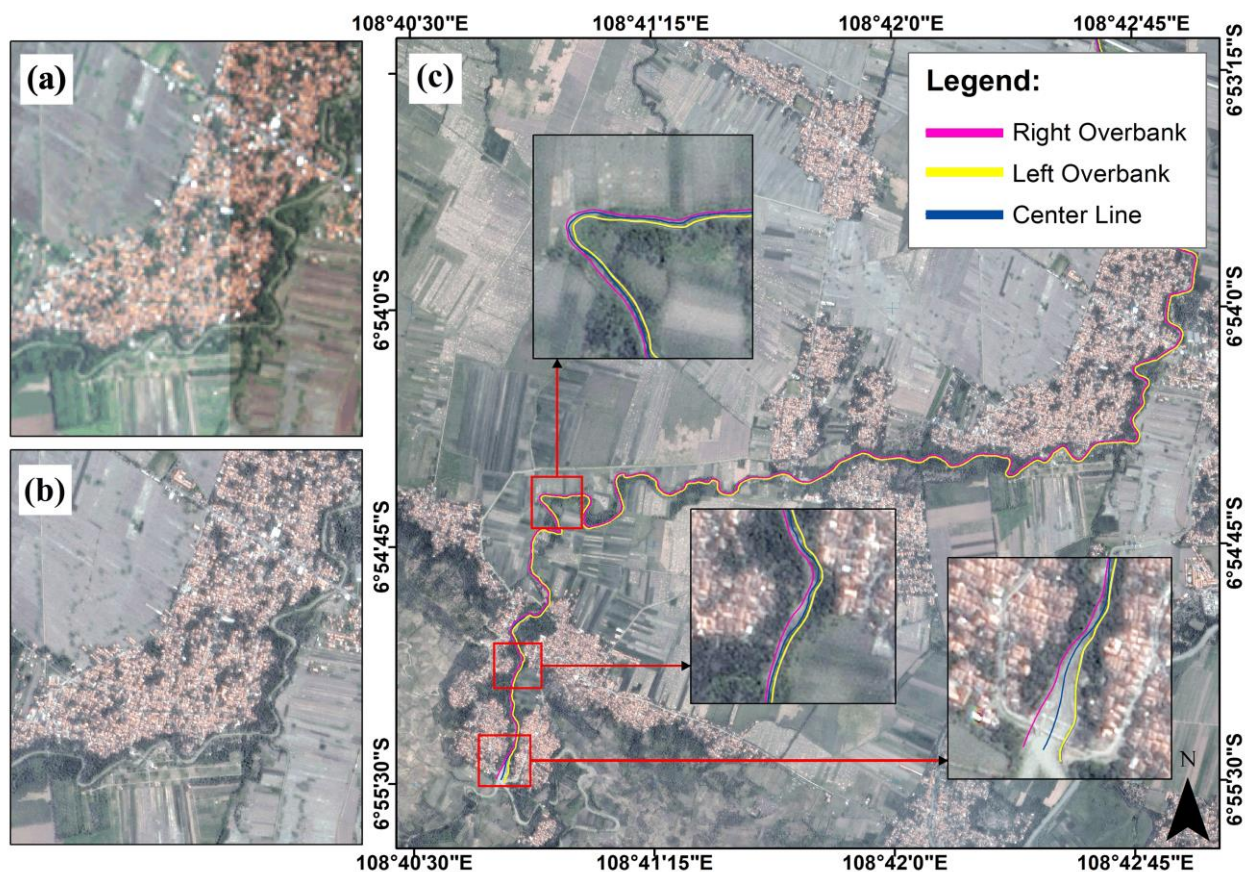

Figure 3. Imagery SPOT 7 processing. (a) Image before pan sharpening, (b) the result of the pan sharpening, and (c) the processing left, right and centre of the river line.

2.2.3. Hydrological Analysis

Hydrological analysis is conducted to estimate the magnitude of flood discharge and is subsequently used as input in creating a flood inundation model due to limitations in streamflow data. Regional rainfall analysis is performed in the upper part of the Ciberes watershed covering an area of 56.22 km2, with a maximum daily rainfall data period spanning 38 years from 1975 to 2012, originating from five rain gauge stations located around the study area (Figure 1). The maximum daily regional rainfall is calculated using isohyets to complete areas uncovered by rain gauge stations. The isohyet method is selected considering the study area's varied topographic conditions, considering the distance between stations and the topographic features. Subsequently, frequency analysis is conducted to calculate the probability of future rainfall using several frequency distribution types, such as Normal Distribution, Gumbel, Log-Normal and Log Pearson III. The appropriate distribution type is determined using Chi-squared and Smirnov-Kolmogorov statistical analyses. Regarding this particular study, the return period selected for rainfall design is the 100-year return period, considering that the 100-year return period is a significant rainfall design period in hydrological studies. It is acknowledged that the values for the 100-year return period are still in the form of daily rainfall. Then, to calculate flood discharge using hydrographs, daily rainfall is transformed into hourly rainfall intensity using the Mononobe method.

Table 1. Cook Coefficient Classification (Meyerink, 1970; Santos *et al.,* 2017)

Watershed characteristics	Characteristics of Runoff Results			
	Extreme Value 100	**High 75**	**Normal 50**	**Low 25**
Relief (Slope)	(40) The terrain has a significant incline, characterised by slope conditions above 30%.	(30) The terrain has undulating characteristics, featuring an average gradient ranging from 10% to 30%.	(20) The terrain exhibits undulating characteristics with a mean gradient ranging from 5% to 10%.	(10) The topography of the region in question is characterised by a relatively even terrain, exhibiting an average gradient ranging from 0% to 5%.
Soil Infiltration	(20) Open ground lacks any form of natural protection, such as rocks or a shallow layer of soil, resulting in an extremely limited ability to absorb water.	(15) The observed phenomenon of a low infiltration rate can be attributed to the presence of clay soil texture or other soil types that possess a limited potential for infiltration.	(10) The soil texture of normal loam, specifically loam soil, exhibits a similarity in infiltration type to that of grassland soil.	(5) In general, a significant proportion of soil exhibits a sandy texture or possesses other soil types that have a high rate of water absorption.
Land Cover	(20) Bare land or areas characterised by extremely limited vegetation coverage.	(15) The presence of natural vegetation is limited, with structures and plants comprising less than 10% of the overall landscape. Additionally, the area exhibits suboptimal drainage conditions.	(10) The area in question has a substantial presence of vegetation, including grass, woody plants or other forms of plant life. However, it is important to note that the vegetation cover does not exceed 50% of the total area, leaving a significant portion of the area devoid of any vegetation.	(5) The vegetation cover in the area is characterised by a high density, with over 90% of the total land area being occupied by various forms of vegetation, including grasses and woody plants.
Drainage Density	(20) The observed phenomenon is characterised by a significant surface depression or flow density exceeding 5 channels per square kilometre.	(15) In typical circumstances, a surface depression, such as a lake, reservoir or marsh, occupies less than 2% of the total drainage area or has a Flow density of 2-5 channels per square kilometre.	(10) The region exhibits a commendable drainage system characterized by a low flow density of less than two channels per Square kilometre.	(5) The area exhibits signs of neglect, with only a limited number of shallow surface depressions and Inadequate drainage capacity.

Generally, rainfall falling on the surface of the Earth can become runoff, intercepted or infiltrated. The calculation of effective rainfall to determine the runoff coefficient that can cause flood events is achieved using the Cook coefficient method. The Cook coefficient method considers four

parameters: relief (slope), vegetation cover, soil infiltration, besides streamflow density (Table 1). Santos *et al.* (2017) mentioned that using the Cook coefficient can be an effective alternative for estimating realistic runoff coefficients in areas with limited hydrological data. The determination of Cook coefficient value classes is completed using spatial analysis in the form of overlay using Geographic Information System (GIS) applications, with a final range of runoff coefficient values from 0 to 1, covering low to extreme values. Thus, the effective rain-fall design intensity is obtained by multiplying the design rainfall intensity value by the runoff coefficient value.

Furthermore, the Snyder-Alexeyev Synthetic Unit Hydrograph is exploited to simulate the flood discharge for the 100-year return period design. Snyder (1938) established empirical relationships for the characteristics of the watershed, specifically the area (A) in square kilometres, length of the river (L) in kilometres, distance from the outlet to the centre of gravity of the hydrological input area (Lc), time lag (h), peak discharge (Qp) in cubic metres per second and time base (tb). The Synthetic Unit Hydrograph can be an alternative method for determining the flow hydrograph at locations where flow measurements are unavailable (Wilkerson & Mer-wade, 2010). The Snyder Synthetic Unit Hydrograph is a commonly exploited method in several countries, including Indonesia. Moreover, certain studies suggest that the hydrograph analysis results closely approximate actual flow hydrographs (Prasad & Pani, 2017). Overall, the definition of a synthetic unit hydrograph is a direct runoff hydrograph (without base flow) recorded at the downstream end of the watershed resulting from effective rainfall of one unit (1 mm) uniformly distributed across the entire hydrological input area in a specified unit of time (Harto, 1993; Natakusumah *et al.,* 2011). Given that the results of the Snyder Synthetic Unit Hydro-graph calculation still represent one unit of flow discharge (1 mm), an analysis of superimposed hydrographs is conducted to obtain a hydrograph curve corresponding to the effective rainfall conditions at the research location.

2.2.4. Two-Dimensional Hydrodynamic Flood Model

Hydraulic analysis performed using HEC-RAS application v.6.4.1 with its RAS Mapper capabilities is used to model floods by spatialising the area, depth and flow velocity. HEC-RAS is hydraulic modelling software commonly used for flood inundation modelling (Vashist & Singh, 2023). Flood inundation modelling is conducted using 2D (two-dimensional) unsteady flow analysis. 2D flood inundation modelling using HEC-RAS can solve the two-dimensional Saint-Venant equation or two-dimensional wave propagation equation (Moghim *et al.,* 2023), allowing it to represent water movement in terms of depth and flow velocity (Vashist & Singh, 2023). This model focuses on the unsteady flow analysis from the upstream (or the beginning of the model-ling) to the lower stream (end of the modelling) because the majority of natural river flow conditions are variable and unstable (Wohl, 2014). Land use data acquired from BBWS Cimanuk-Cisanggarung is used to determine the manning values within the surface runoff coefficient values according to the research conducted by Zahidi *et al.* (2017). HEC-RAS provides various tools that assist in hydrological studies, such as hydrological factors, geometric da-ta correction, river profile (cross-section) editing, Manning coefficients editing, and its RAS Mapper capability.

### 2.2.5. DEM quality assessment for flood simulation

The evaluation of DEM quality in relation to flood inundation modelling is assessed by calculating the RMSE (Root Mean Square Error) and MAE (Mean Absolute Error) values for each modelling result concerning flood depth. The calculation of the RMSE and MAE values is undertaken to determine the quality of modelling based on the level of flood depth. Assessment is carried out by comparing the results of flood inundation depth based on DEM data before filtering and after filtering, as well as DEM arising from the addition of riverbed information with the historical flood depth from field surveys.

3. Results and Discussion

3.1. Filtering Digital Elevation Model

DEM filtering was applied based on the SBF approach, which removes the elevation values from slope in-formation considered objects rather than ground surfaces. The SBF approach emphasises that the dramatic differences in elevation between the two nearest elevation values are not differences in the slope produced by the slope between ground surfaces (Sithole, 2001; Vosselman, 2000; Vosselman & Maas, 2001). The slope angle threshold used is 50%, with a search radius of 30. The search radius is the kernel size employed as input in the search for slope values that fall within the slope angle limit. Determining the kernel radius value is at least half the size of the largest non-ground object to be removed (Vosselman, 2000). Employing this filtering method by applying the slope angle threshold and search radius values, the DEM with slope values equal to

or exceeding the used slope angle limit will be deleted, indicating no more non-ground objects in the DEM. Subsequently, DEM interpolation is performed again to estimate the ground elevation values from the surrounding values using Multilevel B-Spline Interpolation. Multilevel B-Spline Interpolation is an interpolation method developed by Lee *et al*. (1997). This algorithm allows interpolation from coarse to more detailed levels by controlling the structure at each elevation point to decrease the bicubic B-spline function sequentially. As the resulting interpolated DEM still comprises rough features, a smoothing process is performed using the Lee filter with SAGA GIS (Figure 4). The filtering result reveals a maximum elevation value reduction of 13.11 m at the study location.
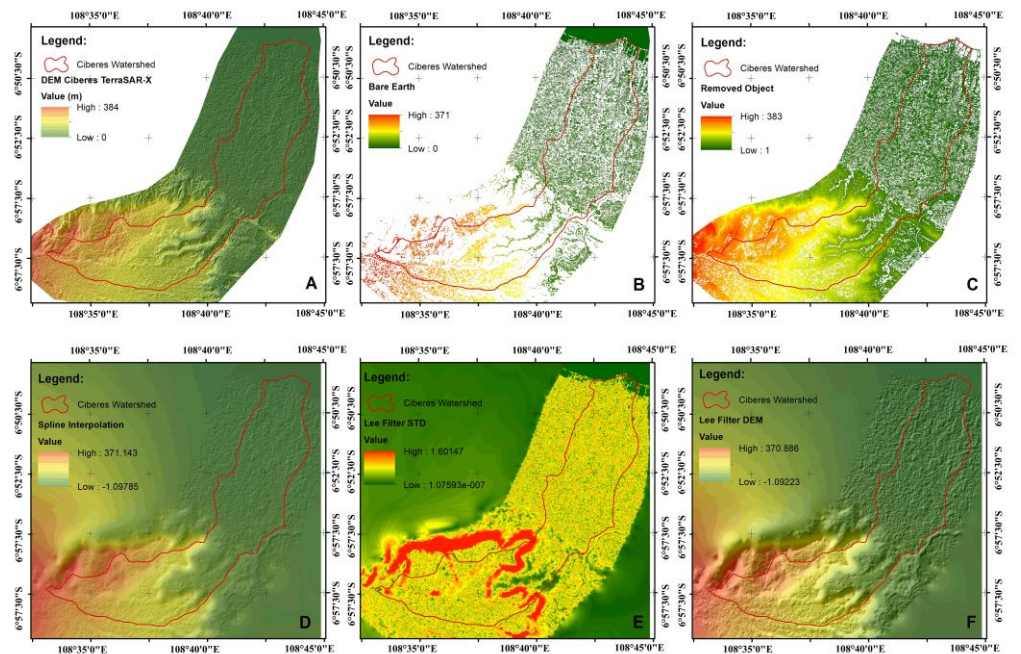
Figure 4. Filtering DEM processing based on slope-based filtering. (A) The original Terra-SAR DEM Product, (B) the pixels referenced as bare earth elevation, (C) the pixel removed as it is not **considered** bare earth because the difference in slope values exceed the threshold, (D) the interpolation process based on the only pixel that recognised as bare earth, (E) and (F) the results from applying Lee filter algorithms to smoothing from coarse to more detailed surface elevation.
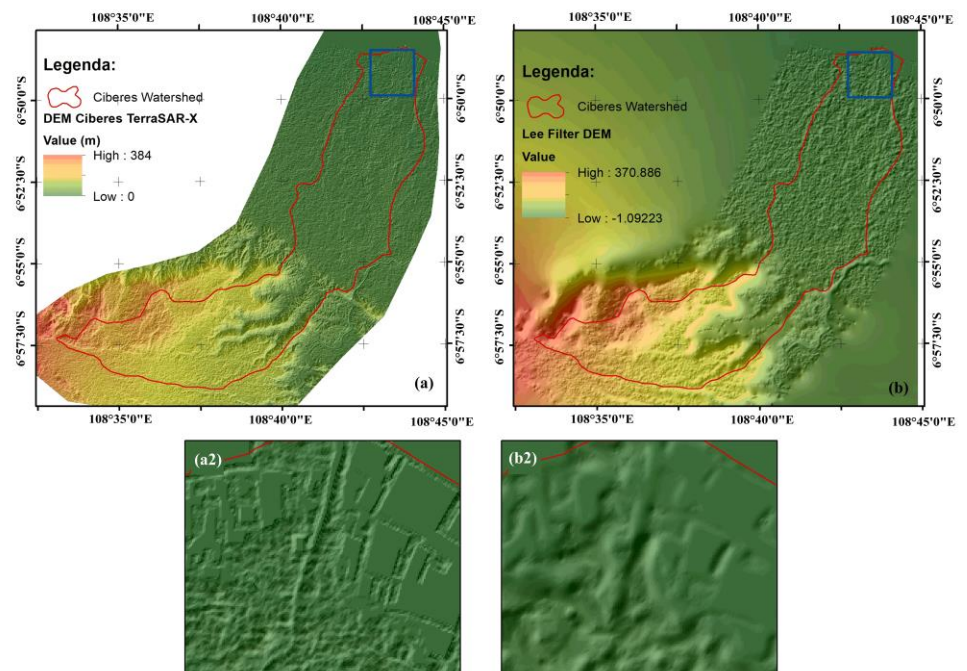
Figure 5. The results of SBF filtering. (a) The DEM before the filtering process, (b) the result of the DEM filtering using the SBF.

Filtering using the SBF method does not deliver the expected results in locations with steep slope gradients as one of the parameters used is the slope gradient with a specific threshold value. Consequently, every location with a slope gradient that falls within the applied threshold value will be assumed to be a non-earth object. Therefore, even if the location is bare earth with a slope gradient within the threshold, it will still be eliminated as a non-earth object. Furthermore, the filtering process also does not deliver the expected results if a cluster of non-earth objects, for example settlements and dense vegetation are merged. The non-earth values that will be eliminated are only in the initial locations where a significant difference in slope is established between the earth and the non-earth objects. Simultaneously, the central areas of vegetation and settlements will be considered bare earth (Chen *et al.,* 2021; Sithole, 2001).

Accuracy testing of the elevation was conducted to assess the accuracy level of the filtered DEM compared to reference elevation points. A comparison dataset of 127 elevation points was obtained from digitising high points on RBI maps with a scale of 1:25,000. The high points on the RBI maps were obtained from detailed aerial photography measurements and had been validated. Thus, they could be used as a reference to assess elevation errors. The RMSE calculations confirmed that the unfiltered DEM had an error rate of 4.11 m, resulting in a LE90 accuracy level of 6.76 m. However, the RMSE value for the filtered DEM indicated an error rate of 3.41, generating a LE90 accuracy level of 5.61 m (Table 2).

Table 2. The calculation of statistical values comparing the DEM data before and after processing

| Statistics	DEM TerraSAR-X (m)	Filtered DEM (m)
Maximum	30	31.02
Minimum	0	0
Standard Deviation	3.18	3.09
RMSE	4.11	3.41
Accuracy E90	6.76	5.61

3.2 Detailing Digital Elevation Model

The cross-section (CS) data acquired from the field measurement of BBWS Cimanuk Cisanggarung, which starts from Bendung Ambit with a length of ± 3.18 km divided into three sections, is utilised as reference data for the vertical accuracy test. The vertical accuracy test of the cross-section across the river aims to determine the level of height difference generated from the DEM data and field measurement data as reference values used for adding the river body area to the DEM. A total of 62 data points were exploited to test the accuracy level of the cross-section derived from the filtered TerraSAR-X DEM (Table 3). The CS data obtained from the field measurement attribute length values to each segment and height values (m) taken based on the reference tie point (BM) to produce height values incorporating greater accuracy. Together with the length and height values, the cross-section in the form of lines in each segment, with each part code already referenced to the coordinates, is also obtained to facilitate accuracy testing. This is undertaken so that both the cross-section obtained from the field measurement and the DEM data obtained have the exact location.

Table 3. Cross-section information based on field survey.

Partition of Cross Section	Cross-Section	Value
Section I	Long	1.10 km
	Mean width	80.78 m
	Max width	102.6 m
	Min width	63.19 m
	Nodes	418
	Total Cross Section	22
Section II	Long	1.08 km
	Mean width	99.60 m
	Max width	130.61 m
	Min width	76.98 m
	Nodes	325
	Total Cross Section	19
Section III	Long	0.98 km
	Mean width	101.48 m
	Max width	115.86 m
	Min width	89.18 m
	Nodes	368
	Total Cross Section	22

The accuracy test was conducted by comparing the elevation values from the reference data with the elevation values obtained from the DEM on the right and left riverbanks and the centreline of the river. The statistical parameters used to test the vertical (height) accuracy level are RMSE and MAE. The test results from the filtered DEM explained that most of the elevation values, both on the right and left riverbanks and in the centre of the river, tend to be higher (Table 4).
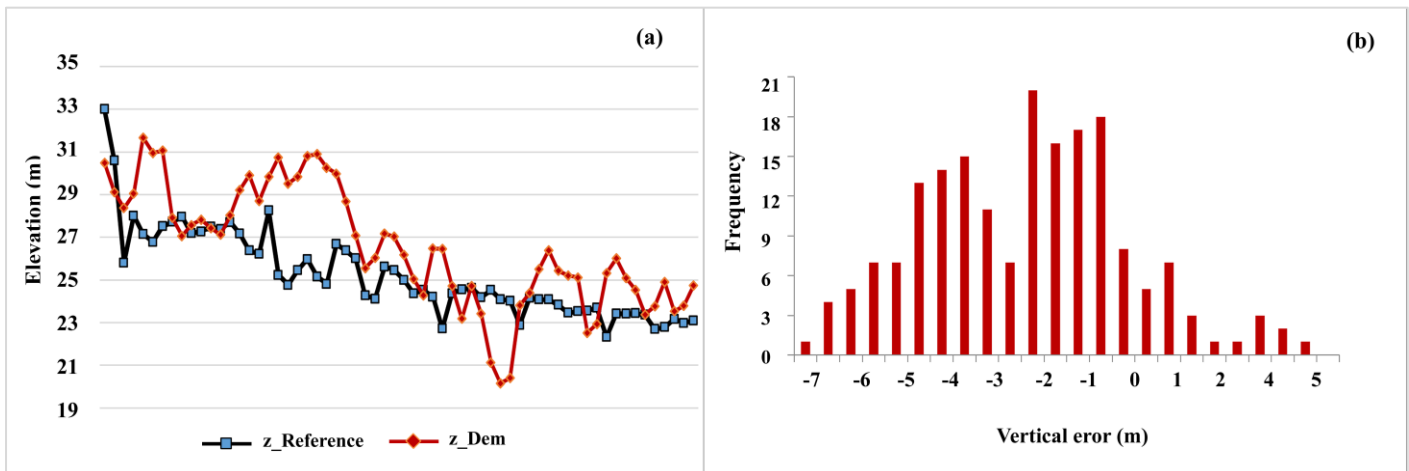
Figure 6. Comparative analysis of elevation discrepancies across riverbanks. (a) The difference in elevation values between the filtered DEM and the reference elevation at the left, right, and centre bank locations, (b) the frequency graph of the difference in elevation values at the left-right and centre.

The results of the RMSE and MAE calculations demonstrate that the level of accuracy of the elevation values from the filtered DEM is ± 4.61 m and ± 4.27 m at the river's centreline, ± 2.51 m and 1.99 m at the left bank, and ± 2.49 m and 2.03 m at the right bank, as shown in Table 4. The Ciberes River's centreline accuracy level is higher than the right-left banks. The difference in elevation values between the centreline and other areas within each cross-section denotes a significant elevation difference. Differences in elevation values will impact the cross-sectional shape related to the channel's capacity and modelling results, including water level and floodplain area if this data is used as topography input in flood modelling. The accuracy level of the elevation at each cross-section influences the discharge flow capacity (Gichamo et al., 2012).

Table 4. The statistical values of the vertical accuracy test results for the river cross-sections on the left and right banks and the middle of the river.

Statistics	River channel (m)	Left Overbank (m)	Right Overbank (m)
MAE	4.27	1.99	2.03
RMSE	4.61	2.51	2.49
Minimum	-7.79	-5.73	-6.00
Maximum	1.26	3.94	4.65
Standard Deviation	1.95	2.14	2.10

Although filtering (DEM filtering) has been carried out in the previous stage to minimise the presence of non-ground elevation values, based on the accuracy test results of the cross-section with the filtered DEM base for the specific area surrounding the river area, it is imperative to perform re-filtering with more detailed data in the river geometry reduction stage. Two factors can cause the difference in elevation values in the DEM. The first is horizontal accuracy, where different places or locations may have different elevations. The second refers to vertical accuracy caused by the recording process that captures non-ground surface information, such as plant height and human-made objects. Several comparisons of cross-sectional profiles between the reference and DEM and the cross-sectional accuracy test process, can be seen in Figure 8.

3.3 Adding River Information

Ordinarily, the level of detail of the TerraSAR-X DEM with a resolution of 9m x 9m is classified as medium-resolution DEM. Hence, the surface appearance of the DEM needs to depict the location of the Ciberes River. Likewise, despite the fact the DEM data has been filtered to remove non-ground elevation values, it still does not show the actual cross-section of the river because the product cannot penetrate the information inside the river. Therefore, further processing is vital to obtain a DEM that includes the river channel location information. The creation of the river channel in the DEM is also essential to ensure its capacity. This guarantees that when flood simulation modelling is undertaken, the flood that occurs in the area around the river results from

exceeding the channel's capacity. The addition of river information is based on the river cross-section accuracy testing results, with MAE values of 4.27 m, 1.99 m and 2.03 m in the middle, left and right areas of the river, respectively. The process of reducing the elevation value information in each part of the river area is illustrated in Figure 7.
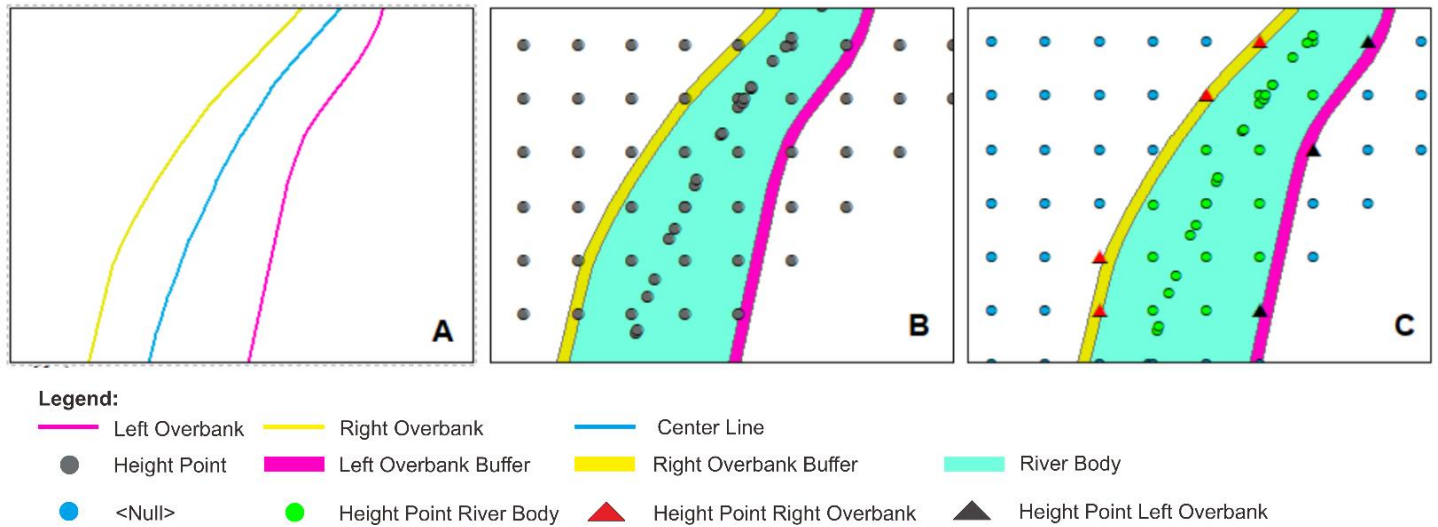

Figure 7. Illustration of reducing the elevation values of height points in the river section.
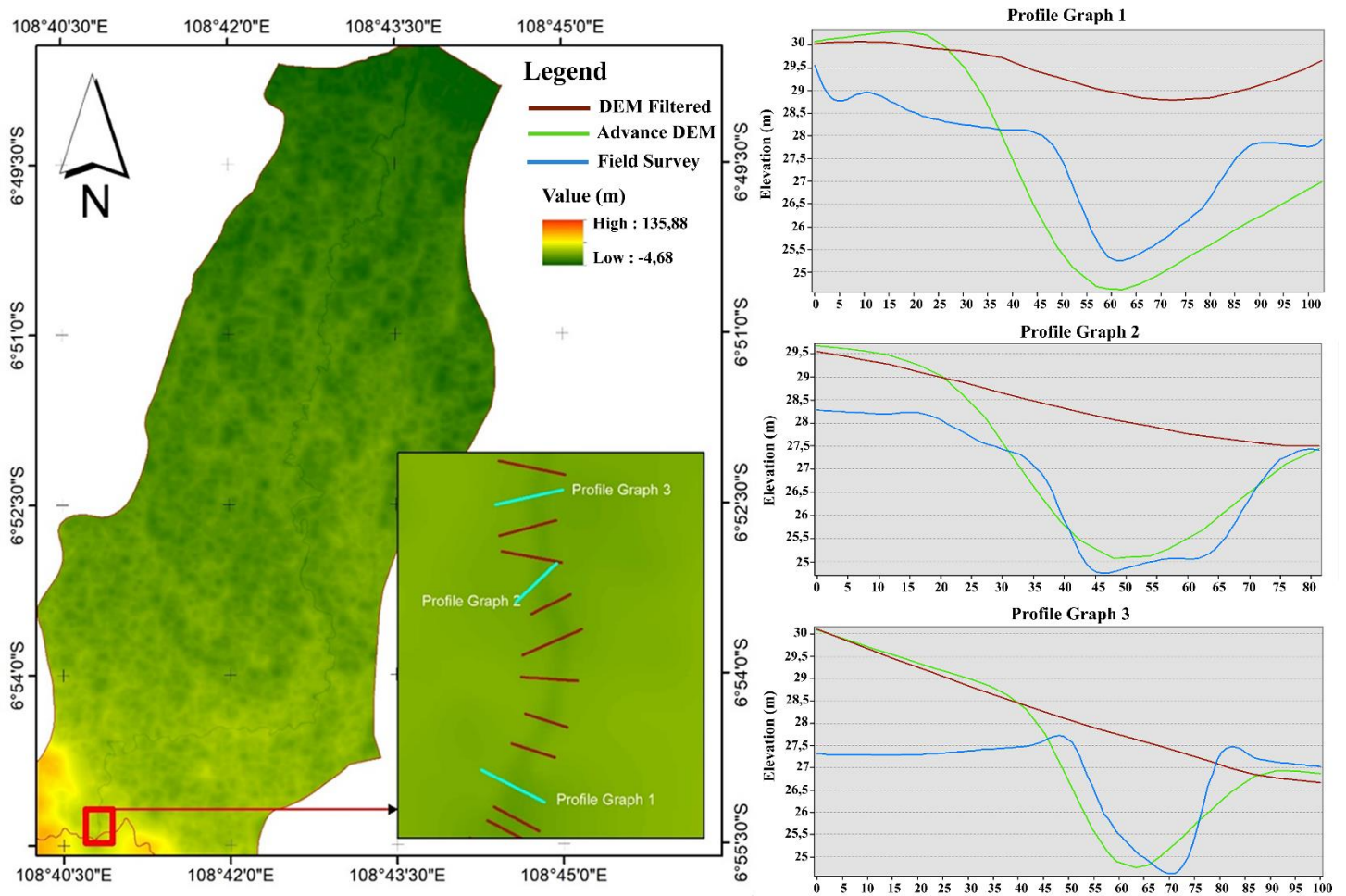

Figure 8. Comparison of river cross-section profiles from filtered DEM, DEM data with added river information, and field measurement data.

Re-interpolation using SAGA GIS software with the multilevel B-spline interpolation method was performed to create a newly developed DEM after adding the river channel information. The

multilevel spline interpolation is an interpolation method developed by Lee *et al.* ([1997](#)). Moreover, the algorithm that belongs to this method allows for interpolation from coarse to finer levels of elevation control at each point to lower the bicubic B-spline function successively. Applying this method also resampled the DEM to a pixel size of 5 m x 5 m to detailing the DEM resolution.

The profile graphs compare the results of the cross-sectional river profiles from the filtered DEM, the new DEM resulting from adding river information and the DEM from the field surveys (see Figure [8](#)). The results of the comparison of the river cross-sectional profiles denote that the river's cross-sectional profile generated from the DEM data, after applying a filter to remove non-ground elevations, fails to portray river morphology, unequivocally failing to represent the depth of the river. Conversely, the river cross-sectional profile generated from the filtered DEM data, incorporating additional river information, realistically represents the river's depth.

Furthermore, the accuracy evaluation of adding river information to the filtered DEM is achieved by comparing the RMSE and MAE values for the three types of river information: left, right and centre of the river (Table [5](#)). The results indicate that filtering has already reduced the differences in elevation values compared to the unfiltered DEM. This improvement suggests an enhanced accuracy in elevation value precision. However, compared to the filtered DEM with added channel river information, it reveals even better accuracy, with MAE values for the right, left and centre being 2.51 m, 2.72 m and 1.91 m, respectively. The increased accuracy in depicting river depth morphology can have a positive impact when used in hydrological applications, particularly flood modelling. Flood events occur when the capacity of the river channel is exceeded. If the input data of the river's capacity reflects the actual field conditions, the excess water during flood modelling represents a natural flood. In contrast, if the river's capacity does not mirror field conditions, it can lead to inaccurate flood extent and depth. Muthusamy *et al.* ([2021](#)) mentioned that the inability of DEM data to represent river channels accurately can result in inaccuracies in flood inundation depth and extent. Filtering DEM data by eliminating non-ground elevation values and adding river channel information to the DEM can be an alternative to improve flood modelling accuracy because DEM data is the primary input for describing not only river channel areas but also the elevation information pertaining to the surrounding floodplain (Casas *et al.,* [2006](#); Muthusamy *et al.,* [2021](#)). River information should be added to flood modelling prior to using DEM data in hydrological applications, notably flood inundation modelling, to ensure that the river's capacity at least approximates field conditions. Preprocessing DEM data in the context of adding river information can also be an alternative to using open-source DEM data with less detailed resolution, such as DEMNAS, NASADEM, SRTM and FABDEM (Forest and Buildings removed Copernicus DEM) to obtain detailed river channel information. Further research regarding DEM data preprocessing can be conducted using open-source DEM data as input to assess its impact when applied to flood inundation modelling.

Table 5. The comparison of the statistical values from the original DEM, filtered DEM and Developed DEM based on information relating to the left, right and centre of the river.

DEM Sources	Left Overbank		Right Overbank		Centre of the River	
	RMSE (m)	MAE (m)	RMSE (m)	MAE (m)	RMSE (m)	MAE (m)
TerraSAR-X DEM	5.39	4.86	5.5	4.98	5.17	4.67
DEM Filtered	4.61	4.22	4.66	4.31	4.63	4.28
Advanced DEM	2.98	2.51	3.22	2.72	2.31	1.91

3.4 Hydrological Analysis

The analysis of regional rainfall is calculated after the daily rainfall data from all observation rain stations have been confirmed for data consistency using a double mass curve. The results of the calculation of regional rainfall using isohyets demonstrate that the minimum regional rainfall amount is 63.44 mm, occurring in 2012. However, the highest regional rainfall occurred in the year 1985, with a total regional precipitation of 137.32 mm and an average regional precipitation value of 92.04 mm (Figure [9](#)). Frequency analysis was conducted to calculate the probability of rainfall magnitudes for the 100-year return period. It was ascertained that the Gumbel distribution is appropriate after suitability tests and chi-squared statistical tests, as well as the Smirnov-Kolmogorov test were performed, for the reason that it has smaller values compared to critical values in other frequency distribution types (Table [6](#)). The calculated rainfall for the 100-year return period is 159.67 mm.

Table 6. Statistical Analysis Determining Distribution Frequencies

| Distribution	Chi-Squared	Chi-Squared Critical Value	Smirnov-Kolmo-gorov	Smirnov-Kolomogorov Critical Value	Results
Normal	13.32	5.99	0.16	0.22	Rejected
Log Normal	7.79	5.99	0.13	0.22	Rejected
Gumbel	5.42	5.99	0.11	0.22	Accepted
Log Pearson III	5.42	3.84	0.09	0.22	Rejected
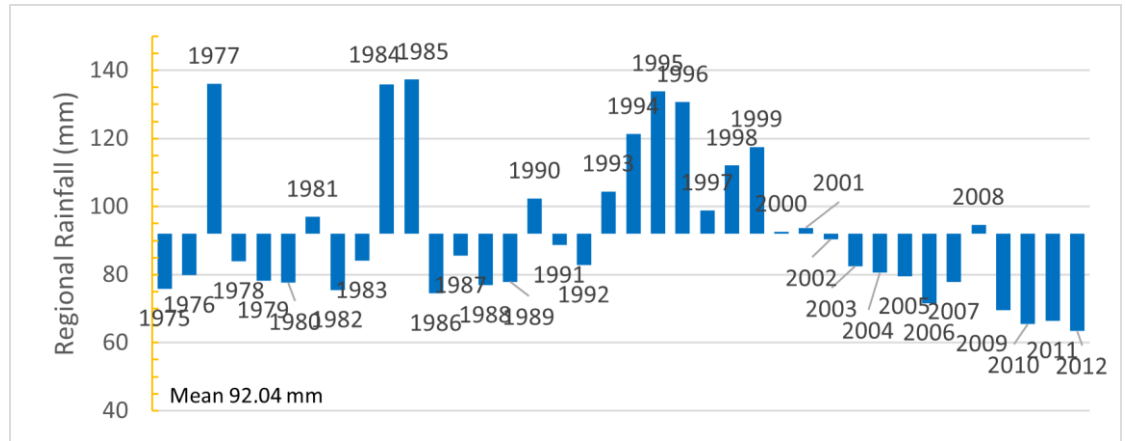
Figure 9. Regional Rainfall over 38 years from 1975 to 2012 in the Ciberes Watershed.

Furthermore, to obtain effective design rainfall, the Cook method uses spatial analysis by overlaying four parameters, specifically relief or slope conditions relating to the hydrological input area, soil infiltration capacity, land cover conditions, in conjunction with flow density conditions. The topographic conditions in the hydrological input area reveal that slopes with a 0 – 5% gradient, classified as flat, dominate with 73%. Subsequently, slope conditions in the 5% - 10% range, classified as a moderate slope, cover 16% of the total area, while the remaining 9% comprises relief types with slopes between 10-30%. The dominant land cover condition in the upstream input area is the rare natural land cover type, comprising 61% of the total percentage, with only roughly 10% representing good land cover conditions in the upstream input area. This is followed by the very rare land cover class, covering 27% of the total area. Regarding the river flow density conditions in the study area, they are dominated by the flow density class <2 channels/km2, covering 61% of the total area, followed by the flow density classes 2-5 channels/km2 and >5 channels/km2, covering 35% and 3% of the total area, respectively. The ensuing parameter is the soil's ability to infiltrate, determined by assessing the soil types in the hydro-logical input area. The soil conditions in the study area are categorised by six soil types: Medi-terranean Brown and Lithosol Association, Grey Alluvial, Brown Latosol and Regosol Association, Greyish Yellow Grumusol and Brown Grumusol Association, Old Grey Alluvial, as well as Latosol and Lithosol Association, covering areas of 67.01%, 14.58%, 12.24%, 5.56%, 0.5% and 0.1%, respectively. The calculation of the flow coefficient is based on the percentage obtained by dividing the area (km2) of each class by the total area of the hydrological input area, which is then multiplied by the accumulated overlay results (Figure 11).
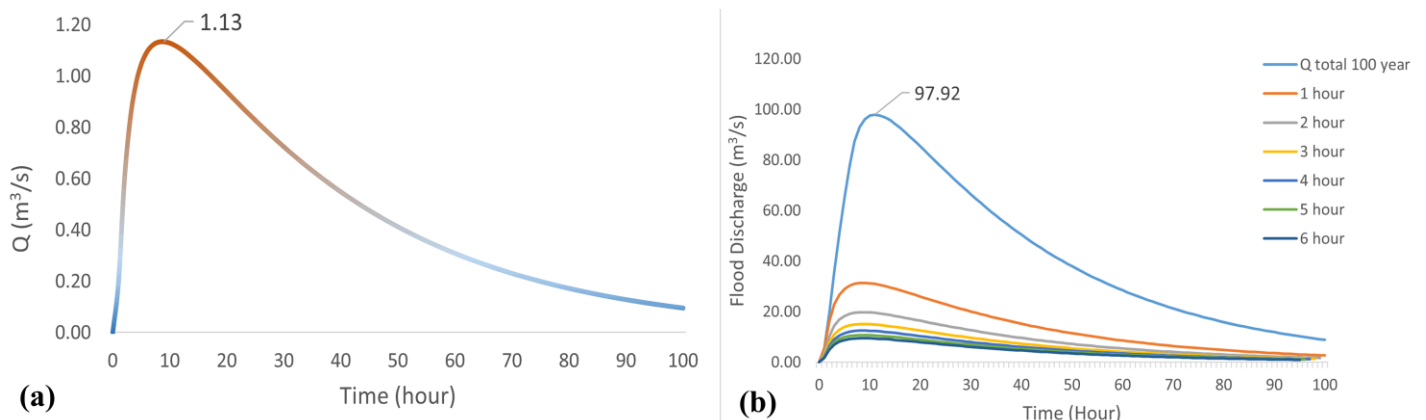
Figure 10. a) The Snyder Synthetic Unit Hydrograph for the input area of the Ciberes Watershed, b) Distribution of flood discharge hydrograph to determine the peak discharge

Based on the calculation results, Manning's roughness coefficient value is 50.19 or 0.5, which is categorised as a normal classification. The flow coefficient for the Ciberes watershed upstream indicates that approximately 50% of the rainfall will be converted into surface runoff and vice versa. The effective 100-year rainfall design is approximately 79.83 mm based on the flow coefficient value. The calculation for the distribution of rainfall design into hourly rainfall was undertaken by means of the Mononobe equation within a period of 6 hours, yielding hourly distribution from 1, 2, 3, 4, 5 and 6 hour values of 27.68 mm, 17.44 mm, 13.31 mm, 10.98 mm, 9.47 mm and 8.38 mm, respectively. Considering the distribution, the average rainfall duration in Indonesia is 5-7 hours/day, and it is completed over 6 hours (Sarido *et al.,* 2008). The creation of the synthetic unit hydrograph by Snyder-Alexeyev, which involves superposition to obtain the distribution of the 100-year rainfall design, reveals that the time to reach the peak flow is 11 hours. Moreover, the magnitude of the peak flow for the 100-year return period is 97.92 m3/s (Figure 10).
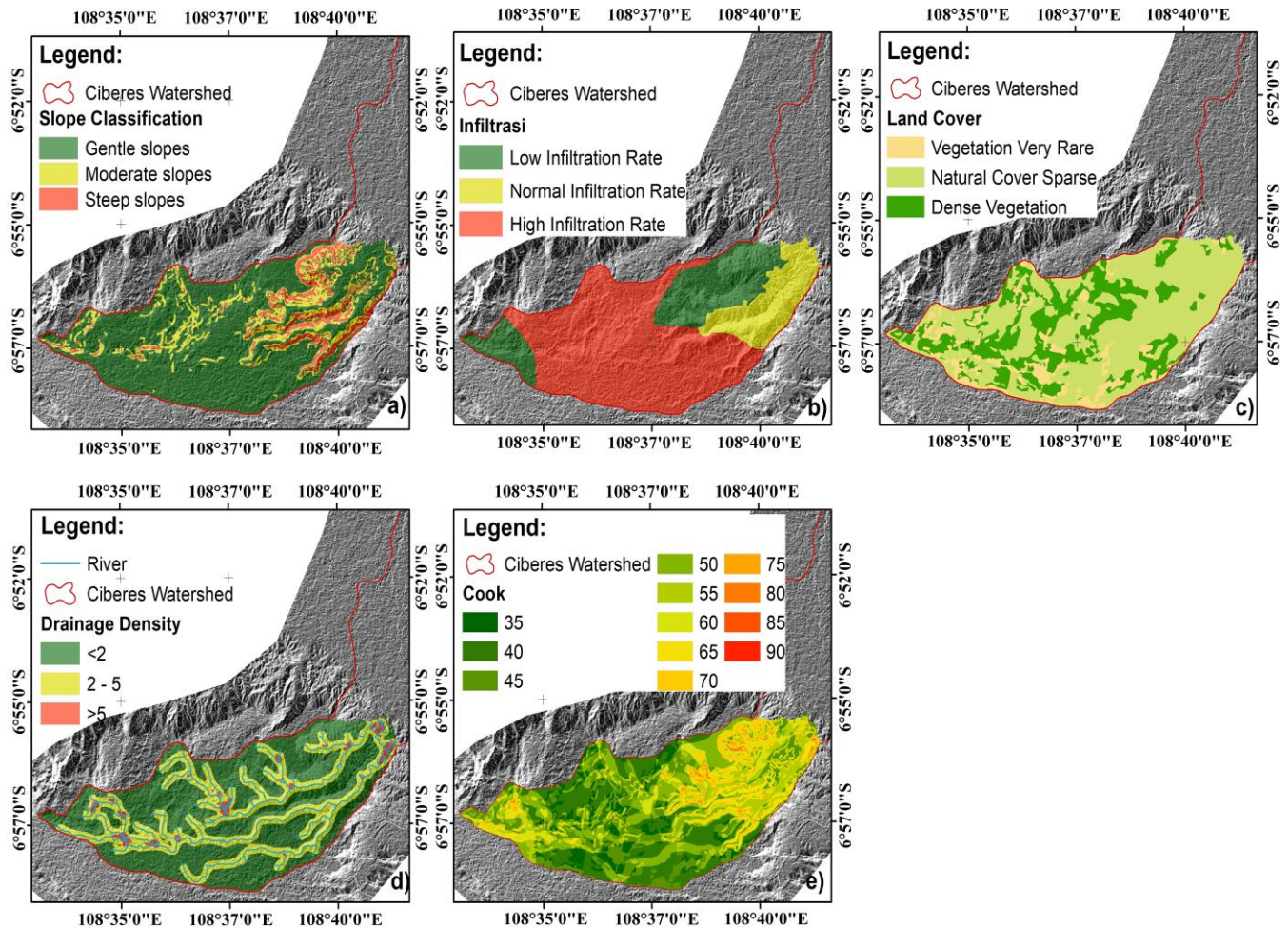

Figure 11. a) Relief condition and its classification on the upper part of the Ciberes Watershed, b) infiltration rate, c) landcover classification, d) drainage density classification, e) Cook value based on four parameters, namely relief, infiltration, landcover and drainage density.

3.5 Two-Dimensional Hydrodynamic Flood Model

Flood modeling results using HEC-RAS consist of raster data, namely flood depth, flow velocity and water surface elevation based on elevation. Each raster cell resulting from flood modelling contains values pertaining to flood depth, flow velocity and water surface elevation. The flood simulation results for the 100-year return period for each type of DEM, namely Ter-raSAR-X DEM, filtered DEM and New DEM, yielded areas of 378.34 ha, 498.63 ha and 639.47 ha, respectively. It is recognised that the differences in the modelled area increase with the processing of the DEM. The difference in flood area between the filtered DEM and original DEM is 24.12%, while the difference in area between the DEM data integrated with river basin information and the original DEM is 40.84%. This difference in area occurs because the loss of non-original elevation information allows for a more likely distribution of floodwater.

Figure 12 illustrates that in the original DEM data, specific areas marked in red (representing rivers) fail to flood owing to elevation factors. This also applies to the filtered DEM data, indicating that the red areas, representing rivers, fail to flood. In contrast, DEM integrated with riverbed information explains that the modelling results follow the river channel with a high depth level in the river area. Additionally, there are differences in the maximum flood depth, with each type of data - TerraSAR-X, filtered DEM and New DEM – comprise maximum flood depths of 8.19 m, 6.97 m and 8.99 m, respectively. The differences in both area and flood depth significantly depend on the elevation level represented by the DEM. Thus, DEM data plays a crucial role in the creation of flood inundation modelling.
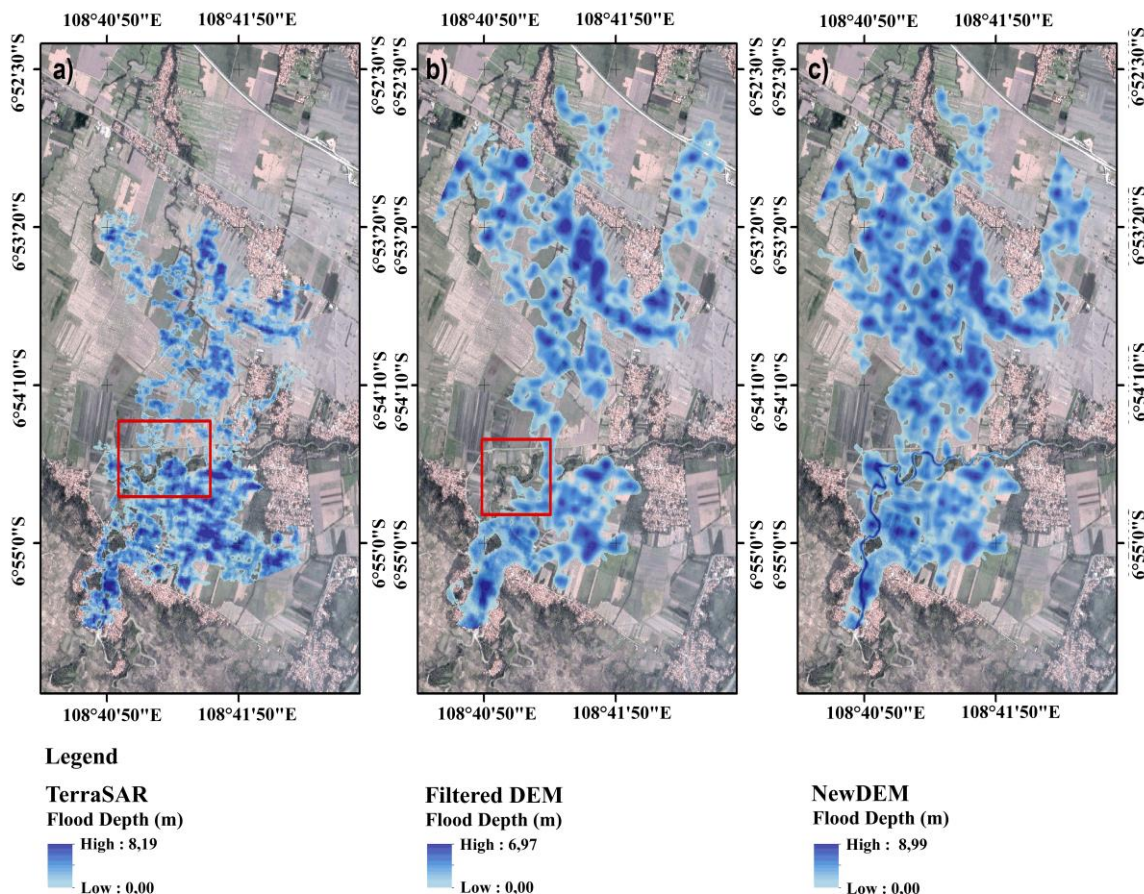
Figure 12. Evaluation of flood modeling techniques tcross different DEM sources. (a) Flood modelling using original DEM TerraSAR-X, (b) Flood modelling using filtered DEM based on the SBF method, (c) Flood modelling using the New DEM integrated with the river bed information based on the river cross-section.

3.6 DEM quality assessment for flood simulation

Based on the flood modelling accuracy assessment results from each application of the DEM data, it was determined that the processing which eliminates non-ground elevations by fil-tering and detailing the riverbed information regarding the DEM could improve the flood depth accuracy level. By comparing flood depth information for each use of TerraSAR-X original DEM data, filtered DEM and New DEM with the field survey, the RMSE values confirmed an increase in accuracy with values of 1.12 m, 0.99 m and 0.84 m, respectively. The filtering process on the DEM removing non-ground elevations using SBF exhibited an increase in flood depth accuracy by 11.67% compared to depth data using the TerraSAR-X DEM without filtering. Nonetheless, increased accuracy in flood depth showed a larger value in the use of the New DEM with a percentage increase in flood depth accuracy of 24.98%. Similarly, the calculation of MAE values in flood inundation modelling using all the DEM data before filtering, after filtering and adding river basin information specifies figures for each data type of 0.87 m, 0.69 m and 0.64 m, respectively. The MAE values for flood depth exhibit results consistent with the RMSE values, signifying that processing undertaken on the DEM can improve accuracy in terms of flood depth.

The increase in flood elevation accuracy in the filtered DEM data shows an increase in the MAE values by 20.70%. Likewise, the process of adding river basin information to the filtered DEM can increase the MAE values by 26.84%. It is important to mention that flood depth information

is essential in flood hazard studies because flood heights > 1.2 m are classified as high-risk levels (Purwandari *et al.,* 2011).

4. Conclusion

Implementation of a filtering method is necessary to obtain a Digital Elevation Model (DEM) that represents the DSM product. This guarantees that elevation information, that is not ground surface, and which might impact the distribution of water flow during floods can be minimised. The accuracy test pertaining to the DEM filtering shows increases in the elevation accuracy from 4.11 m to 3.41 m. Consistent with this, the calculation of the LE90% also showed an increase in elevation accuracy of 1.15 m. Prior to combining the river information, the river profile accuracy test was conducted by comparing the cross-sectional profile produced from the filtered DEM with the field measurement results. The results proved that the accuracy of the centreline of the Ciberes River was more significant than the right and left banks of the river, with RMSE and MAE values of ±4.61 m and ± 4.27 m, respectively. Based on these results, it can be concluded that the DEM product, notwithstanding that it has been filtered, only represents the elevation conditions around the river and not the entire river body, which is the central area of the river. Depth information concerning the river is essential in hydrodynamic flood modelling studies as it is related to the river's capacity to receive water flow. This will significantly impact the distribution and height of floods during modelling.

Therefore, adding river information by reducing the elevation value at the river's right, left and centre is crucial to obtain a cross-sectional river profile corresponding to the field conditions. The accuracy test results of the river's centre, left bank and right bank, with values of approximately 4.27 m, 1.99 m and 2.03 m, respectively, were applied to add river area information. The results of adding river area information can provide a representation closer to the cross-sectional profile of the river based on field measurements within the MAE accuracy level of 2.51 m, 2.72 m, 1.91 m in the left over-bank, right overbank and centre of the river, respectively. Based on the 2-dimensional hydrodynamic flood modelling using HEC-RAS software, every stage of the DEM processing confirms the accuracy of the flood modelling, so as to determine it produces accurate flood modelling. The evaluation was completed by comparing the flood depth based on the non-processed DEM, filtering and adding riverbed information to the filtered DEM data. The results show that removing non-ground elevation utilising SBF could enhance the accuracy of the flood depth from 1.12 m to 0.99 m. The flood depth accuracy in-creases by approximately 11.67% compared to the non-processed DEM. Furthermore, subtracting the river profile information within the filtered DEM could increase the accuracy of the flood depth to 24.98% from 1.12 m to 0.84 m. Equally, the flood depth MAE values explain that the filtered DEM resulted in an accuracy level greater than the non-processed DEM by approximately 20.70%. Furthermore, advanced processing by adding river profile information to the filtered DEM boosted the accuracy to 26.84%. Increasing the accuracy level of the flood depth should significantly impact the flood hazard zonation because the flood depth level is a crucial factor in determining the flood zonation. Purwandari *et al*. (2011) asserted that flood depths higher than 1.2 m will be classified as a high-hazard zone. It is also worth noting that accurate flood mapping is also essential with respect to flood risk management, mitigation, protecting the infrastructure and sustainable planning (Xafoulis *et al.,* 2023).

References

Alfieri, L., Bisselink, B., Dottori, F., Naumann, G., de Roo, A., Salamon, P., Wyser, K., & Feyen, L. (2017). Global projections of river flood risk in a warmer world. *Earth's Future*, 5(2), 171–182. doi: 10.1002/2016EF000485

Ardıçlıoğlu, M., & Kuriqi, A. (2019). Calibration of channel roughness in intermittent rivers using HEC-RAS model: case of Sarimsakli creek, Turkey. *SN Applied Sciences*, 1(9), 1–9. doi: 10.1007/s42452-019-1141-9.

BNPB. (2022). Indeks Risiko Bencana Indonesia (IRBI) Tahun 2022 (Vol. 01). https://bpbd.sukabumikota.go.id/buku-irbi-2022/.

BNPB. (2023). *Data Kejadian Bencana Banjir*. Badan Nasional Penanggulangan Bencana. Retrieved From https://dibi.bnpb.go.id.

Carra, K. A., and Curtin, M. (2017). Posttraumatic Growth Among Australian Farming Women After a Flood After a Flood. Journal of Loss and Trauma, 22, 453–463. doi: 10.1080/15325024.2017.1310506

Casas, A., Benito, G., Thorndycraft, V. R., & Rico, M. (2006). The topographic data source of digital terrain models as a key element in the accuracy of hydraulic flood modelling. *Earth Surface Processes and Landforms*, 31, 444–456. doi : 10.1002/esp.1278.

Chen, C., Guo, J., Wu, H., Li, Y., & Shi, B. (2021). Performance comparison of filtering algorithms for high-density airborne lidar point clouds over complex landscapes. *Remote Sensing*, 13(14). doi: 10.3390/rs13142663.

Chymyrov, A. (2021). Comparison of different DEMs for hydrological studies in the mountainous areas. *Egyptian Journal of Remote Sensing and Space Science*, 24(3), 587–594. doi: 10.1016/j.ejrs.2021.08.001.

Cloke, H. L. (2013). Modelling climate impact on floods with ensemble climate projections. *Quarterly Journal of the Royal Meteorological Society*, 139(671), 282–297. doi: 10.1002/qj.1998.

Author Contributions

Conceptualization: Sahid, S.; **investigation**: Sahid, S; **writing—original draft preparation**: Sahid, S; **writing review and editing**: Sahid, S; **visualization**: Sahid, S. The author have read and agreed to the published version of the manuscript.

Conflict of interest

All authors declare that they have no conflicts of interest.

Data availability

Data is available upon Request.

Danoedoro, P., Gupita, D. D., Afwani, M. Z., Hadi, H. A., & Mahendra, W. K. (2022). Preliminary Study on the Use of Digital Surface Models for Estimating Vegetation Cover Density in Mountainous Area. *Indonesian Journal of Geography*, 54(3), 333–343. doi: 10.22146/ijg.60659.

Elkhrachy, I. (2017). Vertical accuracy assessment for SRTM and ASTER Digital Elevation Models : A case study of Najran city , Saudi Arabia. *Ain Shams Engineering Journal*, 2, 1–11. doi: 10.1016/j.asej.2017.01.007.

Fernandez, A., Black, J., Jones, M., Wilson, L., & Salvador-carulla, L. (2015). Flooding and Mental Health : A Systematic Mapping Review. *PLOS ONE*, 10, 1–20. doi : 10.1371/journal.pone.0119929.

Gichamo, T. Z., Popescu, I., Jonoski, A., & Solomatine, D. (2012). River cross-section extraction from the ASTER global DEM for flood modeling. *Environmental Modelling and Software*, 31, 37–46. doi: 10.1016/j.envsoft.2011.12.003.

Harto, S. B. (1993). *Analisis Hidrologi (1st ed.)*. Penerbit Gramedia Pustaka Utama.

Hawker, L., Bates, P., Jeffrey, N., & Rougier, J. (2018). Perspectives on Digital Elevation Model (DEM) Simulation for Flood Modeling in the Absence of a High-Accuracy Open Access Global DEM. *Frontiers in Earth Science*, 6, 1–9. doi: 10.3389/feart.2018.00233.

Hirabayashi, Y., Mahendran, R., Koirala, S., Konoshima, L., Yamazaki, D., Watanabe, S., Kim, H., & Kanae, S. (2013). Global flood risk under climate change. *Nature Climate Change*, 3(9), 816–821. doi: 10.1038/nclimate1911.

Ihsan, H. M., & Sahid, S. S. (2021). Vertikal Accuracy Assessment On Sentinel-1, Alos Palsar, And Demnas In The Ciater Basin. *Jurnal Geografi Gea*, 21(1), 16–25. doi: 10.17509/gea.v21i1.29931.

Kundzewicz, Z. W., Kanae, S., Seneviratne, S. I., Handmer, J., Nicholls, N., Peduzzi, P., Mechler, R., Bouwer, L. M., Arnell, N., Mach, K., Muir-Wood, R., Brakenridge, G. R., Kron, W., Benito, G., Honda, Y., Takahashi, K., & Sherstyukov, B. (2014). Flood risk and climate change: global and regional perspectives. *Hydrological Sciences Journal,* 59(1), 1–28. doi: 10.1080/02626667.2013.857411.

Kuriqi, A., Koçileri, G., & Ardiçlioğlu, M. (2020). Potential of Meyer-Peter and Müller approach for estimation of bed-load sediment transport under different hydraulic regimes. *Modeling Earth Systems and Environment,* 6(1), 129–137. doi: 10.1007/s40808-019-00665-0.

Lee, S., Wolberg, G., & Shin, S. Y. (1997). Scattered data interpolation with multilevel B-Splines. *IEEE Transactions on Visualization and Computer Graphics*, 3(1), 228 - 244. doi: 10.1109/2945.620490.

Meyerink, A, M. . (1970). *Chapter VII.3 ITC Textbook of Photo-Interpretation in hydrology, A Geomorpholoical Approach (Netherlands (ed.))*. ITC. Retrieved From https://books.google.co.id/books/about/Photointerpretation_in_Hydroogy.html?id=a-owHAAACAAJ&redir_esc=y

Moghim, S., Gharehtoragh, M. A., & Safaie, A. (2023). Performance of the flood models in different topographies. *Journal of Hydrology*, 620(PA), 129446. doi: 10.1016/j.jhydrol.2023.129446.

Muthusamy, M., Casado, M. R., Butler, D., & Leinster, P. (2021). Understanding the effects of Digital Elevation Model resolution in urban fluvial flood modelling. *Journal of Hydrology*, 596. doi: 10.1016/j.jhydrol.2021.126088.

Natakusumah, D. K., Hatmoko, W., & Harlan, D. (2011). Prosedur Umum Perhitungan Hidrograf Satuan Sintetis dengan Cara ITB dan Beberapa Contoh Penerapannya. *Jurnal Teknik Sipil*, 18, 251–291. doi : 10.5614/jts.2011.18.3.6S

Prasad, R. N., & Pani, P. (2017). Geo-hydrological analysis and sub watershed prioritization for flash flood risk using weighted sum model and Snyder ' s synthetic unit hydrograph. *Modeling Earth Systems and Environment*, 3, 1491–1502. doi : 10.1007/s40808-017-0354-4.

Purwandari, T., Hadi, M. P., & Kingma, N. C. (2011). a Gis Modelling Approach for Flood Hazard Assessment in Part of Surakarta City, Indonesia. *Indonesian Journal of Geography*, 43, 63–80.

Sahid, Arifati, A., Nurrohman, A. W., Ihsan, H. M., & Arifin, M. Z. (2017). Vertical Accuracy Assessment for SRTM V.4 and ATER GLOBAL Digital Elevation Models V.2: A Case Study of Padang Regency, West Sumatera. *Seminar Nasional Geomatika* 2017, 399–408.

Santos, F. M. dos, Lollo, J. A. de, & Mauad, F. F. (2017). Estimating the surface runoff from natural environment data. *Management of Environment Quality: An International Journal*, 28, 515–531. doi: 10.1108/MEQ-07-2015-0137

Sarido, L., Hardwinarto, S., & Aipassa, M. I. (2008). Debit Banjir Rancangan dan Kawasan Genangan. *Jurnal KehutananTropika Humida,* 1, 35–48.

Sarkar, D., & Mondal, P. (2020). Flood vulnerability mapping using frequency ratio (FR) model: a case study on Kulik river basin, Indo-Bangladesh Barind region. *Applied Water Science*, 10(1), 1–13. doi: 10.1007/s13201-019-1102x

Sithole, G. (2001). *Filtering of laser altimetry data using a slope adaptive filter*. … Archives of Photogrammetry Remote Sensing and …, XXXIV, 22–24. Retrieved From http://lr.tudelft.nl/fileadmin/Faculteit/ LR/Organisatie/Afdelingenen_Leerstoelen/Afdeling_RS/Optical_and_Laser_Remote_Sensing/Publications/Papers/018-2001/doc/sithole_annapolis.pdf

Snyder, F. F. (1938). Synthetic Unit Hydrographs. *Transactions American Geophysical Union*, 19, 447–454. doi: 10.1029/TR019i001 p00447

Stephenson, J., Vaganay, M., Cameron, R., & Joseph, P. (2014). The long-term health impacts of repeated flood events. *WIT Transactions on Ecology and The Environment,* 184, 201–212. doi: 10.2495/FRIAR140171

Tran, T. N. D., Nguyen, B. Q., Vo, N. D., Le, M. H., Nguyen, Q. D., Lakshmi, V., & Bolten, J. D. (2023). Quantification of global Digital Elevation Model (DEM) – A case study of the newly released NASADEM for a river basin in Central Vietnam. *Journal of Hydrology: Regional Studies*, 45(1), 101282. doi: 10.1016/j.ejrh.2022.101282

Vashist, K., & Singh, K. K. (2023). HEC-RAS 2D modeling for flood inundation mapping: a case study of the Krishna River Basin. *Water Practice and Technology*, 18(4), 831–844. doi: 10.2166/wpt.2023.048

Vosselman, G. (2000). Slope based filtering of laser altimetry data. *International Archives of Photogrammetry and Remote Sensing*, XXXIII(Part B3/2), 935–942. doi : 10.1016/S0924-2716(98)00009-4.

Vosselman, G., & Maas, H. (2001). Adjustment and filtering of raw laser altimetry data. *Proceedings OEEPE Workshop on Airborne Laserscanning and Interferometric SAR for Detailed Digital Elevation Models*, 62–72.

Wilkerson, J., & Merwade, V. (2010). Determination of Unit Hydrograph Parameters for Indiana Watersheds. *Joint Transportation Research Program, September*, 114. doi: 10.5703/1288284314266.

Wohl, E. (2014). Rivers in The Landscape Science and Management (1st ed.). JohnWiley & Sons, Ltd.

Xafoulis, N., Kontos, Y., Farsirotou, E., Kotsopoulos, S., Perifanos, K., Alamanis, N., Dedousis, D., & Katsifarakis, K. (2023). Evaluation of Various Resolution DEMs in Flood Risk Assessment and Practical Rules for Flood Mapping in Data-Scarce Geospatial Areas: A Case Study in Thessaly, Greece. *Hydrology*, 10(4). doi: 10.3390/hydrology10040091.

Zahidi, I., Yusuf, B., Cope, M., Ahmed Mohamed, T., & Mohd Shafri, H. Z. (2017). Effects of depth-varying vegetation roughness in two-dimensional hydrodynamic modelling. *International Journal of River Basin Management*, 16(4), 413-426. doi: 10.1080/15715124.2017.1394313.